Journal of Advanced Research in Natural and Applied Sciences
dergipark.org.tr/en/pub/jarnas
Open Access

ISSN: 2757-5195 12 (3) (2026) 204-232 doi.org/10.28979/jarnas.1902848

A New Approach to Active Tectonics SW of Altınova (Yalova) with Paleoseismological Data, NW Türkiye

Seray Çınar Yıldız [1], Süha Özden [2]

Article Info
Received: 04 Mar 2026
Accepted: 27 Jul 2026
Published: 30 Sep 2026
Research Article

Abstract − This study aims to provide a new perspective on the active tectonics south of the Hersek Delta in the Sea of Marmara based on paleoseismological trenches in the southern part of the North Anatolian Fault Zone. Within this scope, one natural trench was examined at Çavuşçiftliği, immediately southwest of Altınova (Yalova), and a total of five trenches were excavated in Geyikdere and Havuzdere villages. Radiocarbon (^{14}C) dating methods indicate at least five paleo-earthquake events occurred in the region. They may have occurred between AD 66 ± 43 and AD 873 ± 57, AD 873 ± 57 and AD 972 ± 40 in the Geyikdere trenches; AD 1202 ± 32 and AD 1350 ± 30, AD 1350 ± 30 and AD 1359 ± 33, and AD 1359 ± 33 and AD 1875 ± 30 in the Havuzdere trenches. These events may have been related with large earthquakes that likely affected İzmit and surroundings on the northern branch of the North Anatolian Fault Zone. Although a NW–SE directed compressional regime constitutes the main tectonic regime in NW Anatolia currently, ENE–WSW, WNW–ESE and E–W trending normal faults detected in the study area are related to a local NNE-SSW extensional tectonic regime.

Keywords − *Active fault, earthquake, paleoseismology, Altınova, North Anatolian fault*

1. Introduction

The current tectonic regime in the Eastern Mediterranean began with the convergence of the Eurasian, African and Arabian plates during the Middle-Late Miocene, followed by the collision of the Arabian and Eurasian plates in Eastern Anatolia [1-8]. As a result of this collision, the Anatolian plate, located between the Eurasian, Arabian and African plates, has moved westward along two strike-slip faults [1-9]. The North Anatolian Fault Zone (NAFZ) is one of two faults forming the boundary between the Eurasian and Anatolian plates [5-10]. Due to intense seismic activity and status as one of the main tectonic elements in the Eastern Mediterranean region, it is one of the best-known active faults in the world. It extends from Karlıova (Bingöl) in eastern Türkiye to the Northern Aegean Sea (west of Saros Bay) [5]. It is a right-lateral strike-slip fault approximately 1500 km long [9-10]. The NAFZ splays into two branches in the Bolu region [9], known as the northern and southern branches. According to recent Global Positioning System (GPS) studies, the slip rate on the fault varies from ~25 mm/year on the northern branch, starting east of the Marmara Region (Bolu), to ~20 mm/year on the western end (Marmara Sea) [11-13]. The southern branch accommodates horizontal movements on the NAFZ with a slip rate of ~5 mm/year [14]. Geological displacements occurring along the NAFZ since the

[1]seraycinar@gmail.com (Corresponding Author); [2]ozden@comu.edu.tr
[1]School of Graduate Studies, Çanakkale Onsekiz Mart University, Çanakkale, Türkiye
[2]Department of Geological Engineering, Engineering Faculty, Çanakkale Onsekiz Mart University, Çanakkale, Türkiye

Pliocene are not consistent with recent GPS data. This data shows that the slip rate on the northern branch is 3-3.5 times higher than on the southern branch [15].

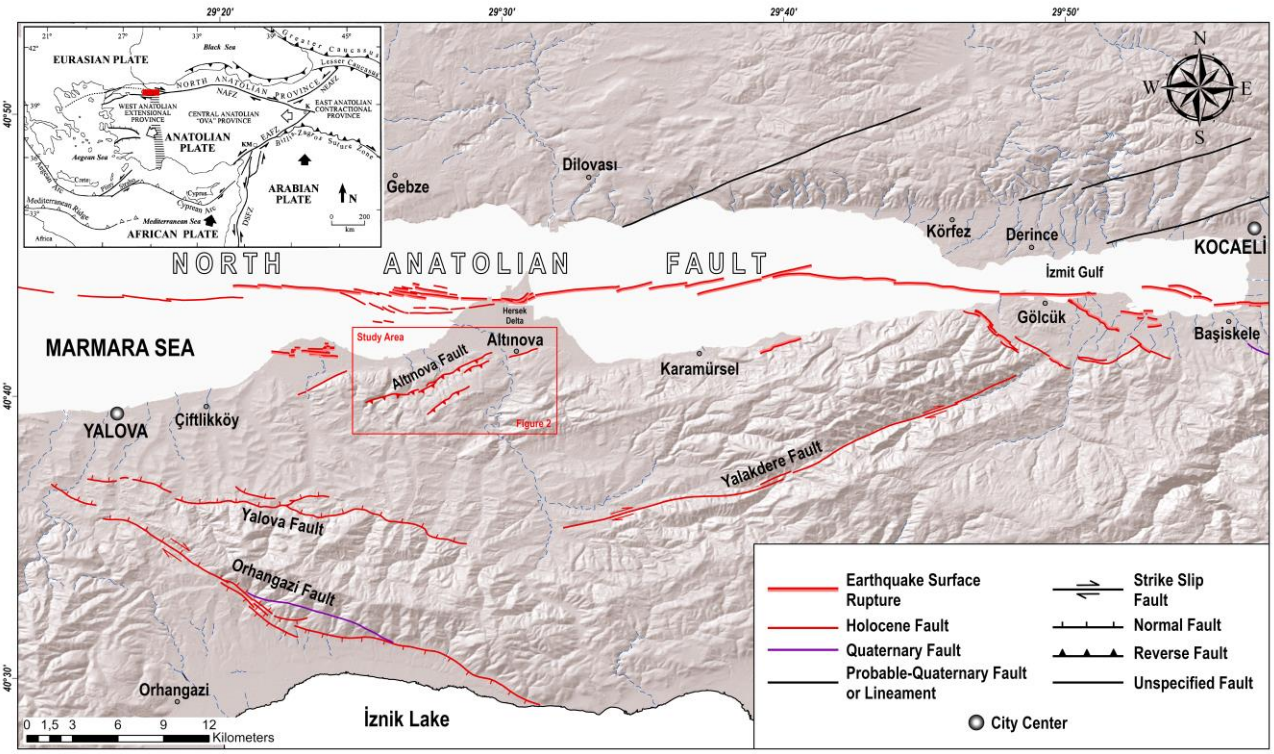


Figure 1. Tectonic map of the study area and surroundings (Modified from [10-19-25]).

The most recent major earthquakes on the northern branch were the Gölcük Earthquake of August 17, 1999 (M_w = 7.4) and the Düzce Earthquake of November 12, 1999 (M_w = 7.2). These earthquakes gave rise to the idea that the earthquake risk in the Marmara Sea section has increased [16-18]. The surface rupture of the August 17, 1999 earthquake ended in the Marmara Sea by cutting the Hersek Delta [19]. Surface ruptures and especially vertical movements indirectly related to this earthquake occurred in terrestrial areas immediately south of the Hersek Delta (rural areas in the region from Yalova to Gölcük). The earthquake history of this region is not sufficiently well known. After the 1999 Gölcük earthquake, many scientists carried out paleoseismological excavations in the Hersek Delta [19-24]. However, no paleoseismological studies have been done to date in terrestrial areas south of this delta. The study area included in this research is located to the south of the Hersek Delta in the Gulf of İzmit (Figure 1). The area is southwest of Altınova district, just south of the northern part of the NAFZ, that passes through the Gulf of İzmit and cut through the Hersek Delta during the August 17, 1999, earthquake. The study area contains the Altınova Fault and its segments, which are defined on the Active Fault Map of Türkiye [25]. This fault and its segments start from the ridges behind Altınova settlement, ~2 km south of the Hersek Delta, and extend in segments along the N60°–70°E direction. The total length of the segments is around 9 km, and they are defined as a thrust faults dipping to the SE [26]. In this study, observations were made of the fault and its segments at two separate outcrops to understand the actual deformation behavior in the region within the investigation area. A total of five paleoseismological trenches were excavated in two areas, and trenching procedures were applied to one natural trench on the Altınova Fault (Figure 2).

The main motivation for this study is the lack of detailed seismic history for the terrestrial areas south of the Hersek Delta. Although there are some records from both historical and instrumental periods about the northern branch of the NAFZ that cuts through the Hersek Delta, the occurrence of significant earthquakes in the study area is unknown. Furthermore, no paleoseismological trench studies have been conducted in this area so far. The characteristics of the faults defined in the region are not compatible with the morphology and surface outcrops in the area. The data obtained from field observations and paleoseismological trench studies will shed

provide information about the dates of past earthquakes and recurrence intervals both in this area and in the Marmara Sea. From another perspective, based on the trench data, new fault characteristics will be presented for the active tectonic behavior in the region and Marmara Sea. All new findings, which include trench profiles, fault types, earthquakes and age determination results, are explained in detail in the results and discussion sections.

1.1. Regional Geology and Tectonics

The metamorphic rock assemblages belonging to the Armutlu–Almacık Zone form the basement unit in the study area. The Armutlu Metamorphics consist of Precambrian metaophiolites and cover rocks located in the west of the Armutlu Peninsula. This basement is equivalent to Paleozoic high-grade metamorphic basement rocks in the İstanbul Zone [27]. The İznik Metamorphics, formed by high-grade metamorphic rocks, are found in the central parts of the Armutlu Peninsula [28]. Permo-Triassic clastic rocks and Late Jurassic–Early Cretaceous rocks are cover units from the Istanbul–Zonguldak and Sakarya zones in the Armutlu Peninsula [27]. These rocks continue upwards with schist, siltstone, sandstone and limestone. Lower–Upper Cretaceous rocks are represented by siltstone, shale, marl and fine-grained sandstone levels [29]. Upper Cretaceous-Eocene units begin with debris flow sediments and shallow marine limestones, with a mudstone, sandstone and marl sequence containing recrystallized limestone and metagranite blocks [27].

Neogene and Quaternary sediments overlie these basement rocks unconformably in the Armutlu Peninsula and Gulf of İzmit region. Neogene sediments are generally found in elevated areas. Quaternary sediments, on the other hand, are emplaced in depression areas developed along the NAFZ [30]. The Neogene sediments in the region consist of Middle–Upper Miocene clastic rocks and Upper Miocene–Pliocene terrestrial clastic rocks. Quaternary sediments are the youngest unit in the region.

The study area is influenced by the NAFZ. This area is located between the northern and southern branches of the NAFZ. In the region, the NE–SW trending strike-slip Yalakdere Fault and the NW-SE trending normal fault character Orhangazi and Yalova Faults are found between the main branches of the NAFZ [25]. In addition, many normal faults in terrestrial areas south of the Hersek Delta were identified in this study (Figure 1).

1.2. Geology of the Study Area

Permo-Triassic clastic rocks form the basement unit in the study area around Altınova in the south of the Gulf of Izmit. This unit, outcropping between Tavşanlı and Taşköprü in the west of the study area (Figure 2), was named the Taşköprü sandstone [31] and consists of sandstone and siltstone. Upper Paleocene–Eocene sedimentary rocks are found in the south of the study area with interbedded volcanic rocks (Figure 2). This unit is observed in large areas in the villages of Kaytazdere, Havuzdere and Geyikdere in the study area. The unit, defined as the Kaytazdere Formation [32], starts with marl at the base and continues with alternations of sandstone and siltstone. Tuffs were deposited in this thick sequence, which generally consists of shallow, sometimes deep marine sediments, by volcanic activity [33]. Middle–Upper Miocene conglomerate-sandstone-mudstone alternations were identified on the north-facing slopes in the study area and are called the Kılıç Formation (Figure 2). This unit consists of gravelly, sandy and silty layers with claystone alternations in places [32]. The calcareous sandstones located in the upper levels of this unit were described as the Yalakdere Formation in the study area. The Upper Miocene–Pliocene Yalakdere Formation overlies the Kaytazdere Formation unconformably. Pleistocene sediments are found in the north of the study area and in the valleys extending along streams (Figure 2). These sediments consist of marine terraces and alluvium. The terraces are located at approximately 40–55 m above sea level and were defined as the Altınova Formation [32]. This formation generally consists of loosely cemented Ostrea sand, clayey sand, silty sand, marl, sandy marl and

Cerastoderma sand levels. It is widely found in hills extending in a north-south direction around Çavuşçiftliği village. This sequence overlies the Yalakdere Formation with an angular unconformity (Figure 2).

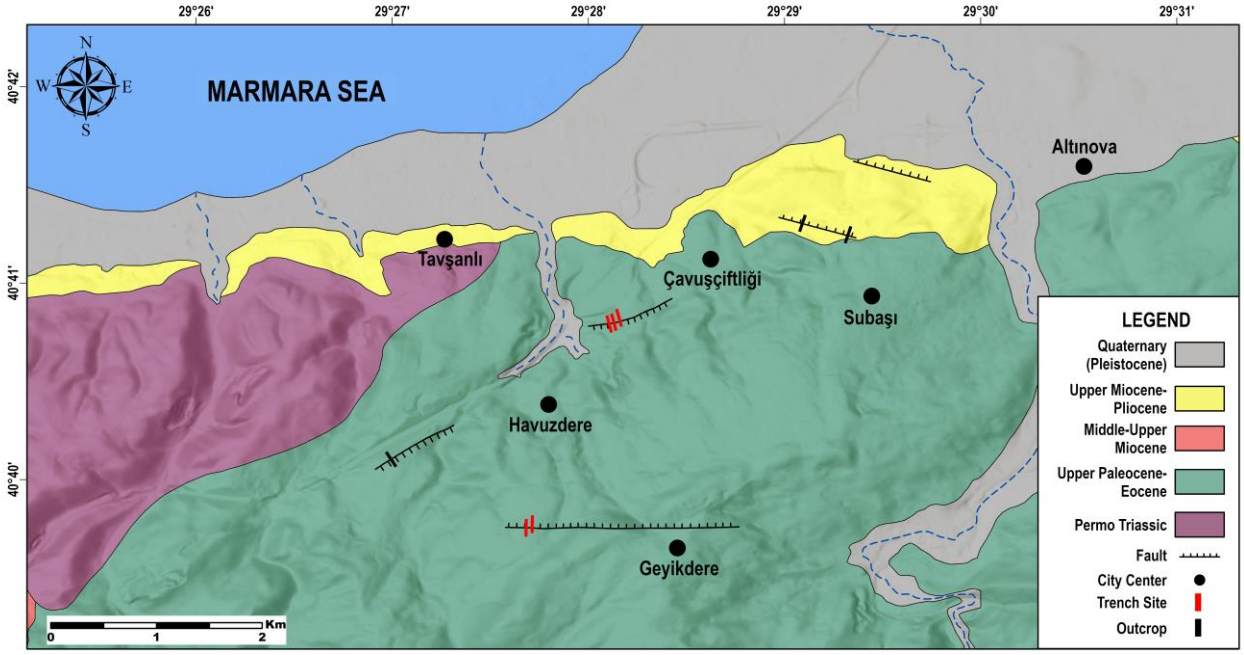


Figure 2. Geological map of the study area (modified from [31]).

1.3. Seismicity of the study area and its vicinity

Earthquakes in the Marmara Sea and surroundings are known date back to the third century BC [34]. Historical seismic records exist for this region, centered around İstanbul, the capital of both the Byzantine and Ottoman empires [34-35]. Seismic activity in the Marmara Region is shown in Figure 3. Earthquake records covering two thousand years show that, on average, at least one moderate (M~6) earthquake occurs every 50 years and a major earthquake occurs every 300 years [18].

Destructive earthquakes in the Marmara Region have occurred along both branches (in north and south) of the NAFZ in historical and instrumental periods. Furthermore, major earthquakes are more concentrated and exhibit a more linear pattern along the northern branch. Earthquakes have occurred at longer intervals in large areas on the southern branch of the Marmara Region.

According to historical records, devastating earthquakes occurred in the Gulf of İzmit and eastern Marmara region on the northern branch in AD 268, AD 478, AD 554, AD 989, AD 1296, AD 1332, AD 1719, AD 1754 and AD 1878 [36-38]. Two major earthquakes affected the region during the instrumental period on September 18, 1963 (M_w = 6.1) and August 17, 1999 (M_w = 7.4). The Izmit Earthquake, centered in Gölcük-İzmit, caused a surface rupture of approximately 145 km with a lateral displacement of between 1.5–5 m, consisting of five segments from west to east: Hersek, Karamürsel–Gölcük, İzmit–Sapanca Lake, Sapanca–Akyazı and Karadere [19].

Within the study area, there are two earthquakes recorded during the instrumental period: one with a magnitude of M_w 2.6 in the Çavuşçiftliği locality on September 24, 1994, and another with a magnitude of M_w 2.7 east of Geyikdere on November 9, 1993 (Figure 3). This data indicates that there is weak seismic activity in the study area over the past 125 years.

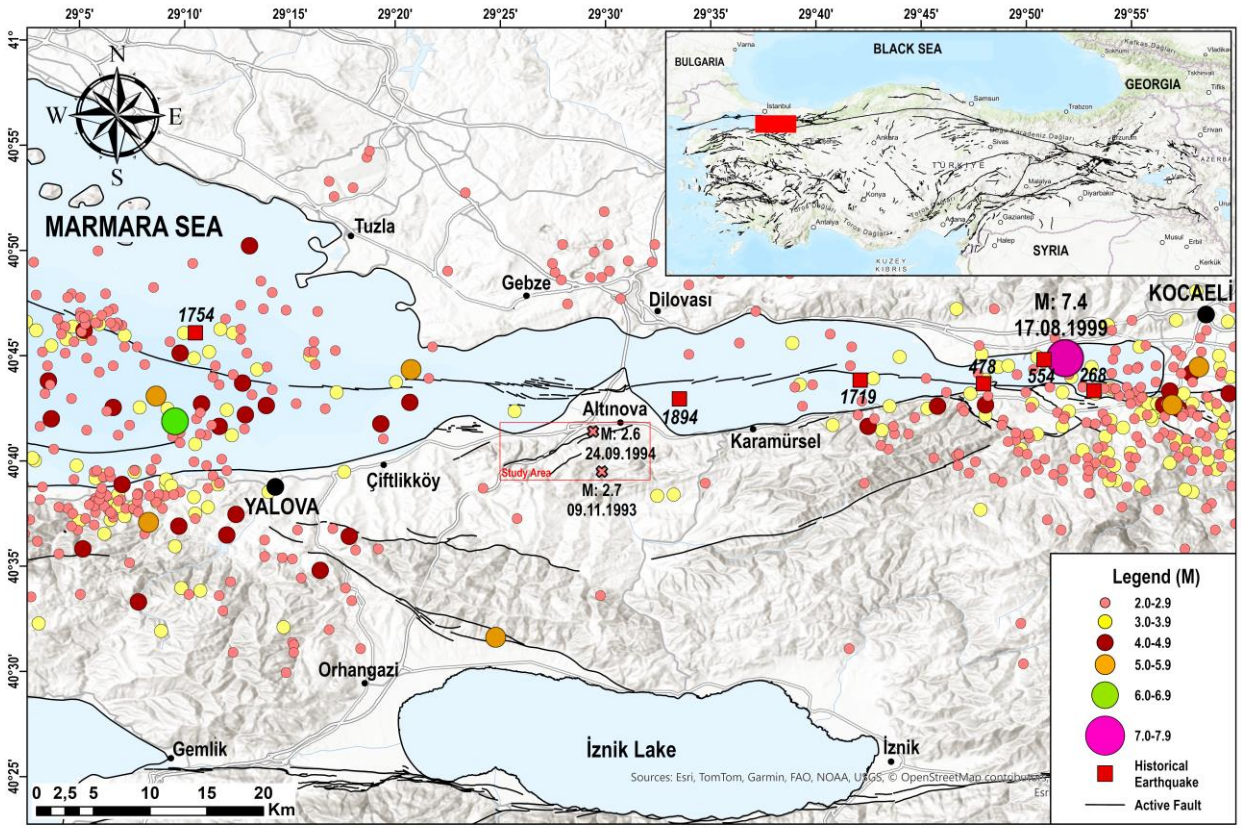


Figure 3. Distribution of historical and instrumental earthquakes in the study area and surroundings.

2. Methods

2.1. Ground Penetrating Radar (GPR)

This method can be used on the boundaries of geologic formations, unit changes and faults, and can detect grain size (clay, sand, silt), porosity ratios, and water contents based on the differences in electrical properties [39-41]. In this method, the signal that is reflected and deformed by layer boundaries, faults, unconformities and/or buried objects is recorded as a function of the arrival time at the receiving antennae [42]. The obtained radar data are presented as cross-sections similar to the seismic method. Amplitude values are extracted from all measurements for a certain time value and plotted on the measurement points on the map [41].

2.2. Paleoseismological trench study

Paleoseismological studies are conducted by excavating trenches across active faults to identify past earthquakes. These studies included trench excavation, leveling and wall cleaning, grid mapping, photographing features, photomosaic creation, logging and sampling. Samples were taken from the layers related to paleoearthquakes (event horizons) in the excavated trenches for ^{14}C and OSL analyses in order to identify and date these events and stratigraphic layers.

2.3. Radiocarbon dating

Radiocarbon dating (^{14}C) is a widely preferred method for determining the age of ancient organic materials [40-41]. It is based on the principle of radioactive decay, particularly the decay of ^{14}C isotopes in organic matter. Living organisms absorb carbon from the atmosphere, including trace amounts of radioactive ^{14}C. When death occurs, this absorption stops, and ^{14}C within the organism decays to nitrogen-14 (^{14}N) at a known

rate with a half-life of approximately 5730 years [43]. This predictable decay rate forms the basis of ^{14}C radiocarbon dating, allowing the age of organic samples to be calculated using mathematical formulas [44]. The ^{14}C samples taken in this study were dated at the TÜBİTAK–MAM Earth Sciences Accelerator Mass Spectrometry (AMS) Laboratory.

2.4. Optical Luminescence Dating (OSL)

OSL has become an important tool to date sediments of interest in paleoseismological research. Data obtained from luminescence dating can be used to determine unit age, time of faulting, calculate slip rates and estimate earthquake recurrence intervals. In geological settings, luminescence allows estimation of the time elapsed since the last exposure of sand and silt grains to sunlight; this exposure is assumed to have occurred during sediment transport. Therefore, the luminescence age is the deposition age of the sediment. Currently, the standard method for luminescence geochronology in paleoseismic research is quartz single-aliquot regenerative-dose (SAR) OSL because quartz can be easily bleached [45] and the SAR method provides a routine procedure for multiple luminescence measurements [46]. The OSL samples taken in this study were dated by Ankara University Earth Sciences Research and Application Center (YEBİM).

3. Results

Normal faulting was observed at natural trenches in three different regions. Paleoseismological trenching procedures were applied to one of these. Additionally, a total of five trench studies were conducted at two different locations. The MTA (Mineral Research and Exploration Institute) active fault map of Türkiye [26] was used to primarily determine trenching locations, and both lithological and structural elements were investigated in the field. Ground penetrating radar studies were conducted to two potential locations in Geyikdere and Havuzdere villages (Figure 4).



Figure 4. Locations of observed outcrops and paleoseismological trenches excavated within the study area.

The Buzhane site (Universal Transverse Mercator [UTM] 35T: 710769 E / 4507514 N) is located 1 km southwest of Altınova district. This area was uncovered during excavations for the foundation of a cold storage facility. The Upper Miocene-Pliocene Yalakdere Formation and the Pleistocene Altınova Formation were

observed in the Buzhane natural excavation. This natural trench is oriented in N74°W direction, with approximately 15 m length and 5 m depth. A normal fault with N40°E strike and 40°SE dip was found in this outcrop wall, displacing calcareous sandstone layers by approximately 1 m (Figure 5). The slip striations on the fault have 62°W direction.



Figure 5. Normal fault (N40°E, 40°SE, 62°W, Dextral Normal; A-A': 1 m) observed at the Buzhane location.

The Büyükbalkan Çiftliği site (UTM 35T: 707709 E / 4505312 N) is located on a hill 500 m west of Havuzdere village and 1.5 km south of Tavşanlı town. This hill contains a tuff member of the Upper Paleocene-Eocene Kaytazdere Formation. The Büyükbalkan Çiftliği trench is oriented in the N75°W direction, with approximately 20 m length and 6-6.5 m depth. Fault planes are clearly observed in the wall, and a vertical displacement of approximately 20 cm is clearly visible at the current ground level (Figure 6). The fault has N48°E direction with 70°SE dip, and the slip striations are in the 80°W direction. These data indicate that the faulting has normal character with a small right-lateral component.



Figure 6. Fault planes and slickenlines observed at the Büyükbalkan Çiftliği location.

3.1. Paleoseismological Studies

In this study, a total of 6 trench studies were carried out in 3 different areas. They are named the Çavuşçiftliği, Havuzdere and Geyikdere trenches. Trench profiles, trench walls, geological features of trenches, faults and fault wedges associated with these faults and earthquake dating results are presented in this section. ^{14}C dating was performed on 21 samples from these trenches. The calibrated ages were calculated with the Oxcal v4.4.4 program [47-48]. Table 1 presents these dates.

Table 1. ^{14}C dating data obtained from samples taken from the Altınova trenches.

Altınova Trenches			
AFH - Çavuşçiftliği Natural Trench			
Samples Code	**TÜBİTAK-MAM Age**	**Calibrated Age (cal AD / BC)**	**Material Type**
AFH1-C01	7444 ± 39	6317 ± 52 BC	Bulk
AFH1-C03	8162 ± 43	7168 ± 76 BC	Bulk
AFH1-C04	6865 ± 37	5750 ± 44 BC	Bulk
GDH - Geyikdere Trenches			
Geyikdere 1			
GDH-D-C02	1391 ± 26	AD 642 ± 19	Bulk
GDH-D-C03	1957 ± 28	AD 66 ± 43	Fault wedge
GDH-D-C04	3639 ± 32	2012 ± 59 BC	Bulk
GDH-D-C07	1501 ± 32	AD 575 ± 36	Fault wedge
GDH-D-C08	1165 ± 30	AD 873 ± 57	Bulk
Geyikdere 2			
GDH2-CO1	1068 ± 29	AD 972 ± 40	Fault wedge
GDH2-CO2	1614 ± 32	AD 474 ± 42	Bulk
GDH2-CO3	1203 ± 31	AD 826 ± 50	Fault wedge
HDH - Havuzdere Trenches			
Havuzdere 1			
HDH1B-C02	4656 ± 34	3448 ± 47 BC	Bulk
HDH1B-C03	577 ± 29	AD 1359 ± 33	Fault wedge
HDH1B-C04	9061 ± 38	8273 ± 28 BC	Bulk
Havuzdere 2			
HDH2-C01	849 ± 26	AD 1202 ± 32	Bulk
HDH2-C02	4380 ± 32	2996 ± 63 BC	Bulk
HDH2-C03	604 ± 30	AD 1350 ± 30	Bulk
Havuzdere 3			
HDH3-C01	150 ± 30	AD 1875 ± 30	Fault wedge
HDH3-C02	1322 ± 27	AD 711 ± 41	Bulk
HDH3-C03	602 ± 27	AD 1350 ± 30	Bulk
HDH3-C04	1100 ± 26	AD 945 ± 36	Bulk

Table 2. Summary of interpreted paleoearthquake events and supporting paleoseismological evidence from the Geyikdere and Havuzdere trenches.

Trench	**Event**	**Interpretation Criteria**	**Evidence**	**Maximum Age Constraint**	**Minimum Age Constraint**	**Event Correlation**
Geyikdere 1	E1	Fault termination + colluvial wedge	Fault displaces Unit 1 and terminates upward at the event horizon. A colluvial wedge was deposited immediately after faulting and subsequently sealed by Unit 2.	AD 66 ± 43	AD 642 ± 19	-
	E2	Fault termination + colluvial wedge	Faulting displaced Units 1 and 2, producing a younger colluvial wedge that is overlain by Unit 3.	AD 575 ± 36	Recent soil	-

Geyikdere 2	E1	Fault termination + colluvial wedge	The event is expressed by upward termination of the fault within Unit 1 and the subsequent deposition of a colluvial wedge, which is overlain by Unit 2.	AD 474 ± 42	AD 972 ± 40	GD1-E1
	E2	Fault termination + colluvial wedge	A younger surface-faulting event displaced Units 1 and 2 and generated a colluvial wedge that is sealed by Unit 3.	AD 82 6± 50	Recent soil	GD1-E2
Havuzdere 1	E1	Fault termination + colluvial wedge	Two fault strands displace Units 1–3 and terminate upward at the event horizon. One fault is associated with a well-developed colluvial wedge, indicating a surface-faulting earthquake.	3448 ± 47 BC	AD 1359 ± 33	-
Havuzdere 2	E1	Fault termination	A single fault offsets Units 1–3 and terminates beneath Unit 4, indicating a surface-faulting event that predates deposition of Unit 4.	2996 ± 63 BC	AD 1202 ± 32	-
	E2	Fault termination + colluvial wedge	Two fault strands terminate immediately beneath the present ground surface. One strand is associated with a colluvial wedge, suggesting a younger surface-faulting event subsequently sealed by modern soil.	AD 1350 ± 30	Recent soil	-
Havuzdere 3	E1	Fault termination	A fault offsets Units 1 and 2 and terminates beneath Unit 3, indicating that faulting occurred prior to deposition of Unit 3.	AD 711 ± 41	AD 1350 ± 30	HD2-E1
	E2	Fault termination + colluvial wedge	Fault 3, which intersects units 1 and 2, terminates within the unit, forming a wedge.	AD 1350 ± 30	AD 1875 ± 30	HD2-E2
	E3	Fault termination + colluvial wedge	The westernmost fault offsets Unit 3 and is sealed by the modern soil, indicating the youngest surface-faulting event recognized in the trench.	AD 1875 ± 30	Recent soil	

3.1.1. Çavuşçiftliği Trench

The Çavuşçiftliği location (UTM 35T: 710226 E / 4507246 N) is situated 2 km southwest of Altınova district and 1 km northeast of Çavuşçiftliği village. Faults were observed in a natural corridor extending N50°E on top of this hill, which is approximately 50-55 m above sea level. The 16 m long and 4 m high trench consists of a marine terrace composed of alternating layers of sand with high fossil content and thin layers of gravelly sand with varying sizes (Figure 8). There are four faults with vertical displacements in the northeast direction at meters 1, 8, 11 and 13 from the southwest of the wall. In the first 10 m from the west of the trench wall, there are deposits consisting of alternating layers of fine-grained sand and well-to-medium sorted fine-to-medium-grained gravel, with grey–beige color. The upper sections of these visible strata contain a level of coarse-grained, poorly-sorted sand matrix gravel approximately 15 cm thick. This is followed by another layer of fine-grained gravel and sand. Between the 11th and 15th meters of the trench, sandy sediments with high density of fossiliferous layers are found. The sediments begin at lower levels with fine-grained fossiliferous sands in shades of grey-beige and yellow, and include a level where medium-grained gravels are concentrated in a thin band. Following this, there is another layer of fine-grained sand and fossils. It continues upwards with a level containing coarse gravel, rounded and angular blocks. These sediments are overlain by fine-grained sandy-silty deposits ranging in color from yellow and light brown to whitish with occasional carbonate additions. The fault designated as F3, located at 120°/50°N, forms a boundary between the initial alternating units and these later sediments. In the western part of the section, although the fossil-bearing fine-grained sands are in a thin layer, they lie above the gravel-sand alternation, so these vertical movements were interpreted as due to normal faults. The material that appears to have washed away on the terrace is thought to have been transported or artificially filled in (Figure 8).

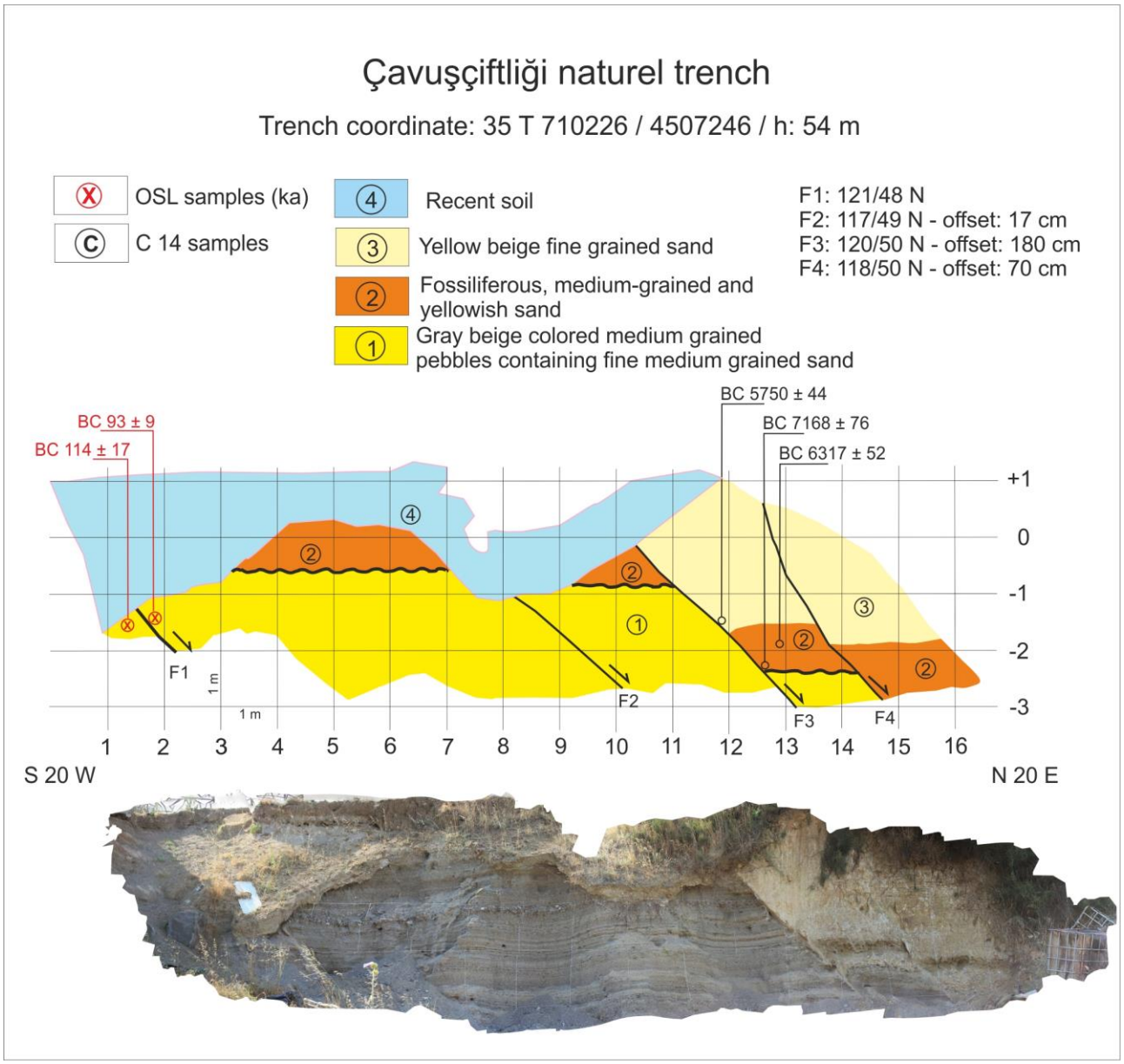


Figure 8. Log and photomosaic of the Çavuşçiftliği outcrop.

The ^{14}C dating results from right side of the trench (around F3 fault) represent 7168 ± 76 BC, 6317 ± 76 BC and 5750 ± 44 BC. These dating results provide the ages of the horizontally-oriented stratigraphic levels. In the west side of section (around F1 fault), OSL age dating (ka) results of 114 ± 17 BC and 93 ± 9 BC corresponds to the ages of the stratigraphic level. These results show that the F3 fault, which cuts the youngest stratigraphic level in the trench, is younger than 5750 ± 44 BC and is covered by recent soil level above it. No dating could be made for the uppermost recent soil level. Radiometric dating results from the Çavuşçiftliği outcrop show that F3 normal fault is an active fault segment and also no evidence of earthquakes was present (Figure 8).

3.1.2. Geyikdere Trenches

Two trenches were excavated (UTM 35T: 708455 E / 4503790 N), 550 m northwest of Geyikdere village at this location, on the southern segment of the fault designated as the Altınova Fault. A GPR survey was conducted first in the area where excavation was planned (Figures 9-10). Measurements were taken along a 40 m line oriented NNW–SSE. The presence of faults was detected at meters 10 and 16 of the profile.

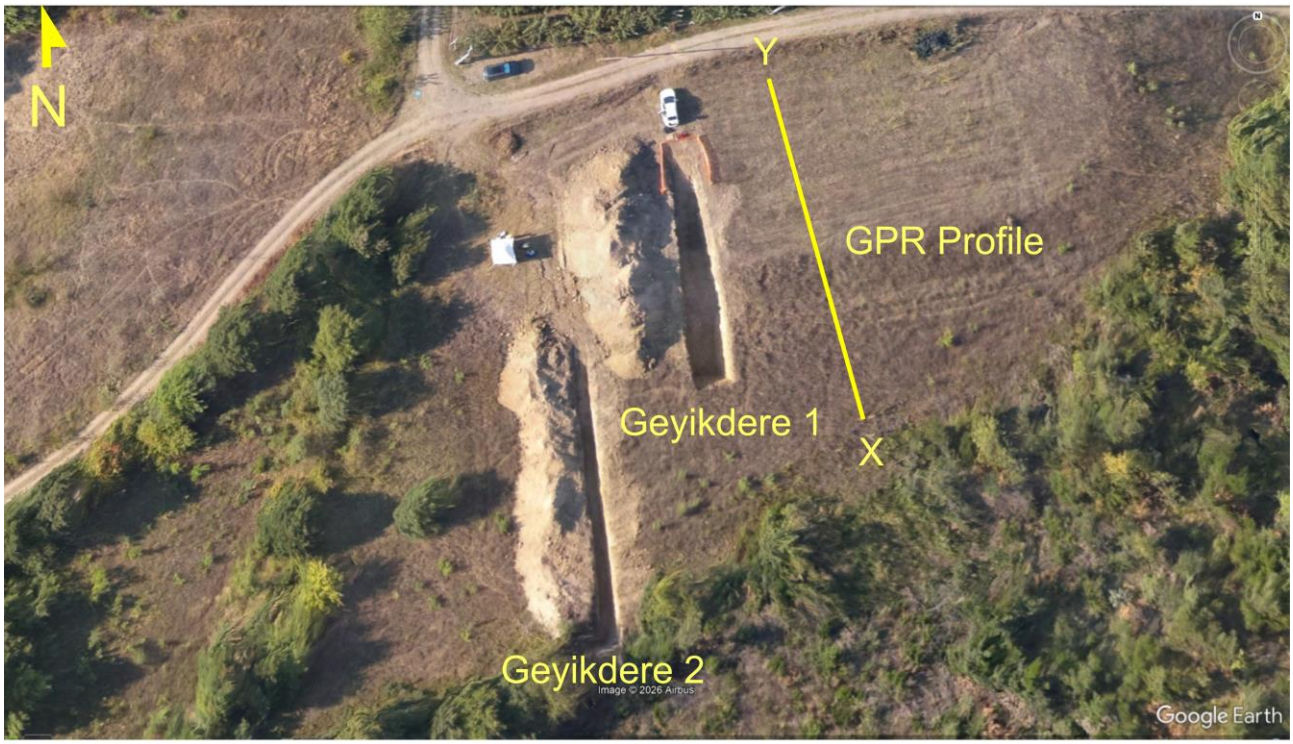


Figure 9. View of Geyikdere GPR profile and trenches.

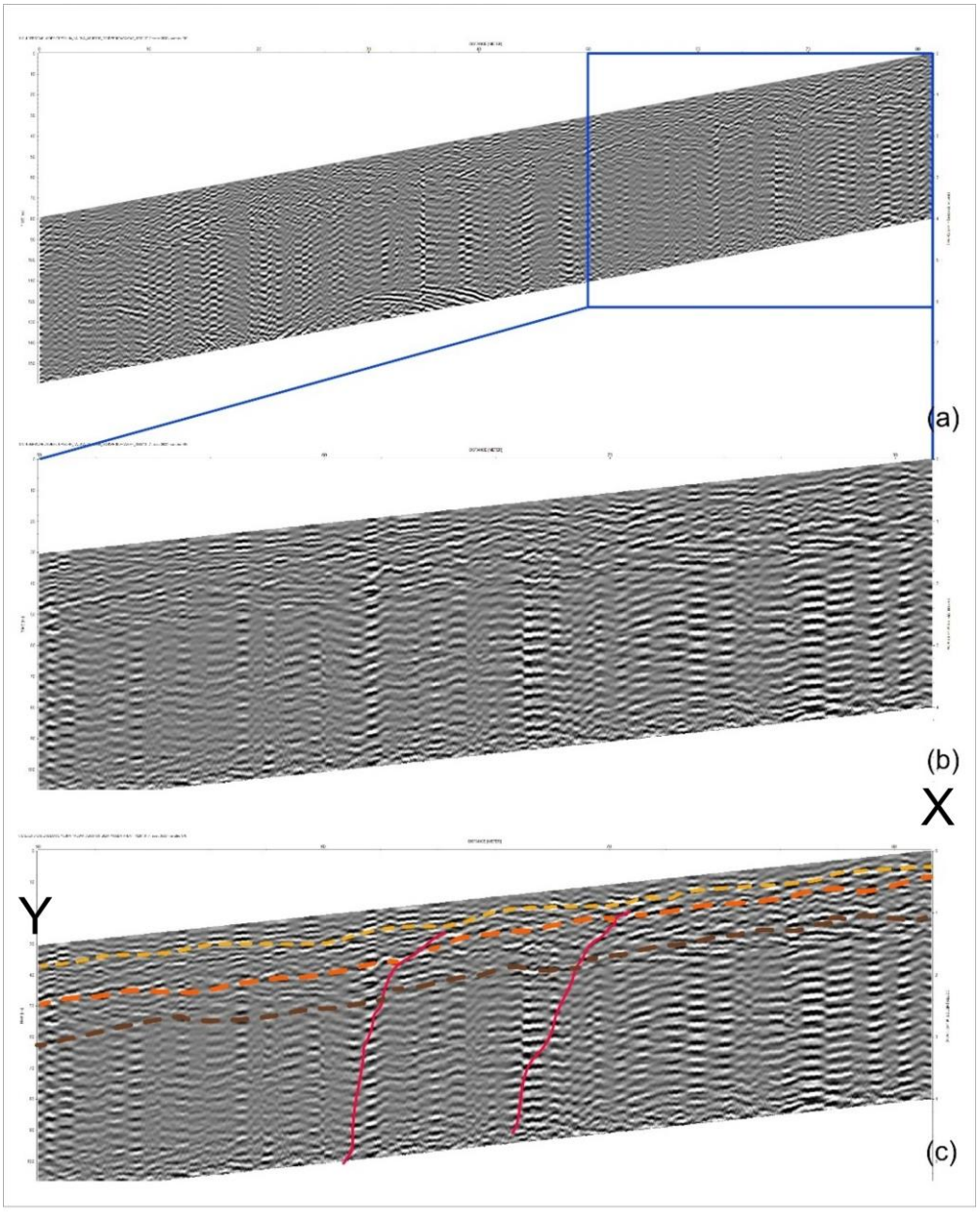


Figure 10. GPR measurements in the Geyikdere Trench area; (a) Processed GPR data (b) Anomaly region representation (c) Modeled GPR data (dashed lines indicate possible layer boundaries, red lines indicate possible discontinuity regions).

Geyikdere Trench 1 is 19 m long, 2.5 m wide, and 3 m deep. Three stratigraphic units are distinguished in the trench walls along with the recent soil level. At the base is fine-grained clayey sand (Unit 1) containing yellow-beige, white tuff and green andesite volcanic rock fragments. Fine-to medium-grained clay and fine-grained sand observed above this are yellowish-brown in color (Unit 2). Both units contain angular, large pebbles and blocks of volcanic origin. The sequence is covered by the recent soil level (Unit 3). Faults are located at 90°/45° N at the 9th meter and 90°/50° N at the 13th meter to the north (Figure 11). There is a fault wedge on each fault.

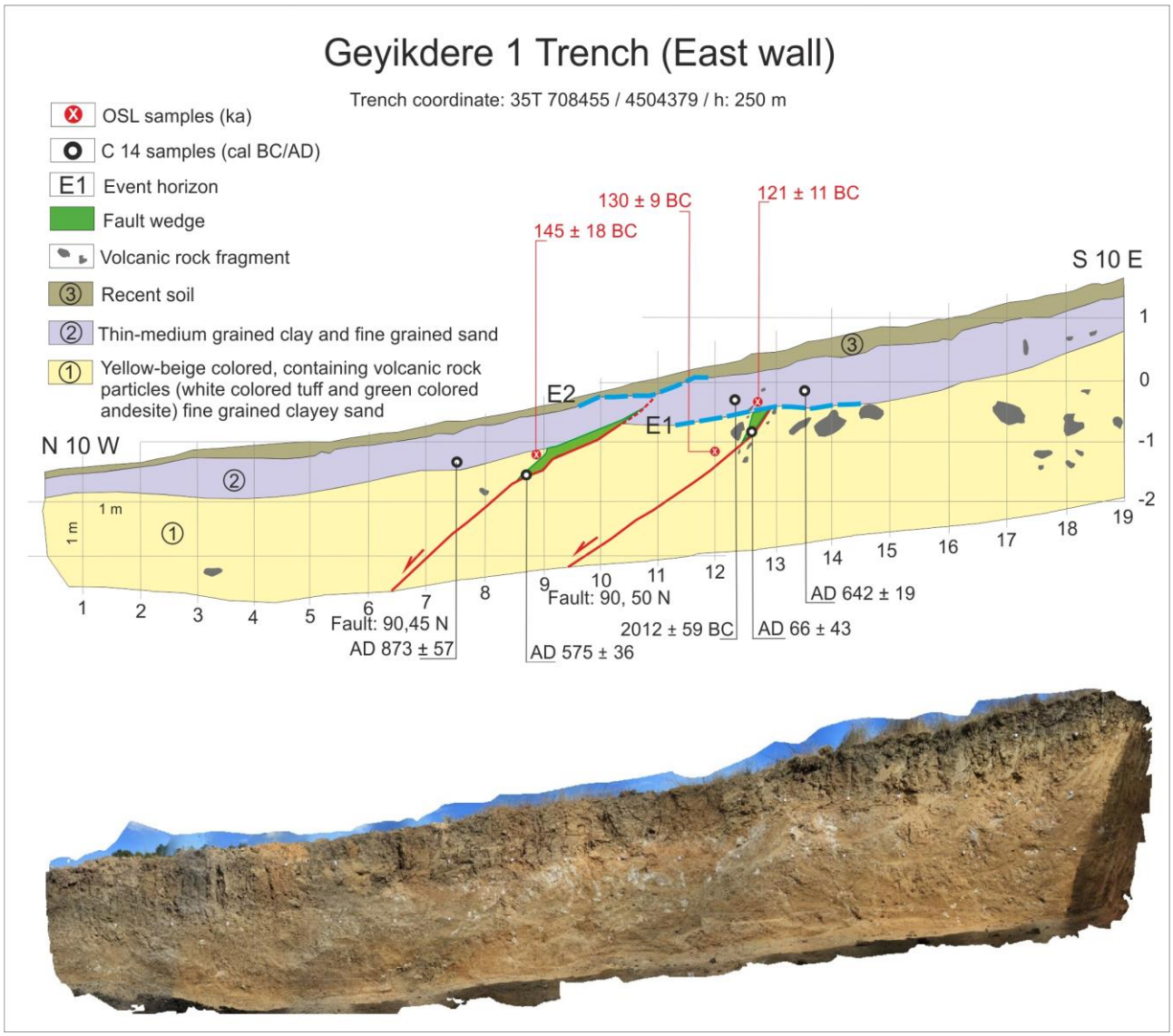


Figure 11. Log and photomosaic of Geyikdere 1 Trench.

Eight samples were taken for OSL and ^{14}C dating (Figure 10). According to the ^{14}C dating results from this trench, two earthquakes were dated to occur between AD 66 ± 43 and AD 642 ± 19 (E1 horizon) and between AD 575 ± 36 and recent soil (E2 horizon). The OSL data (ka) 121 ± 11 BC, 130 ± 9 BC and 145 ± 18 BC were considered unit ages in the trench.

The Geyikdere 2 Trench was excavated to a length of 16 m, a width of 1.5 m, and a depth of 2 m. Three units were identified in the trench walls, including the current soil level. Grey–beige clayey sand at the base of the trench and above it is light brown fine-grained sand. It is covered by the current soil level. Three faults were identified in the trench wall: 4 m from the north at 90°/70° N, 9 m at 90°/60° N and 13 m at 90°/60° N (Figure 12). Fault wedges are present on the trench wall.

According to the ^{14}C dating results from the Geyikdere 2 trench, three samples were dated to AD 972 ± 40, AD 826 ± 50 and AD 474 ± 42. The OSL data (ka) are considered to be unit ages of 56 ± 5 BC and 70 ± 8 BC (Figure 12). Two earthquakes were dated to occur between AD 474 ± 42 and AD 972 ± 40 (E1 horizon) and between AD 826 ± 50 and recent soil (E2 horizon).

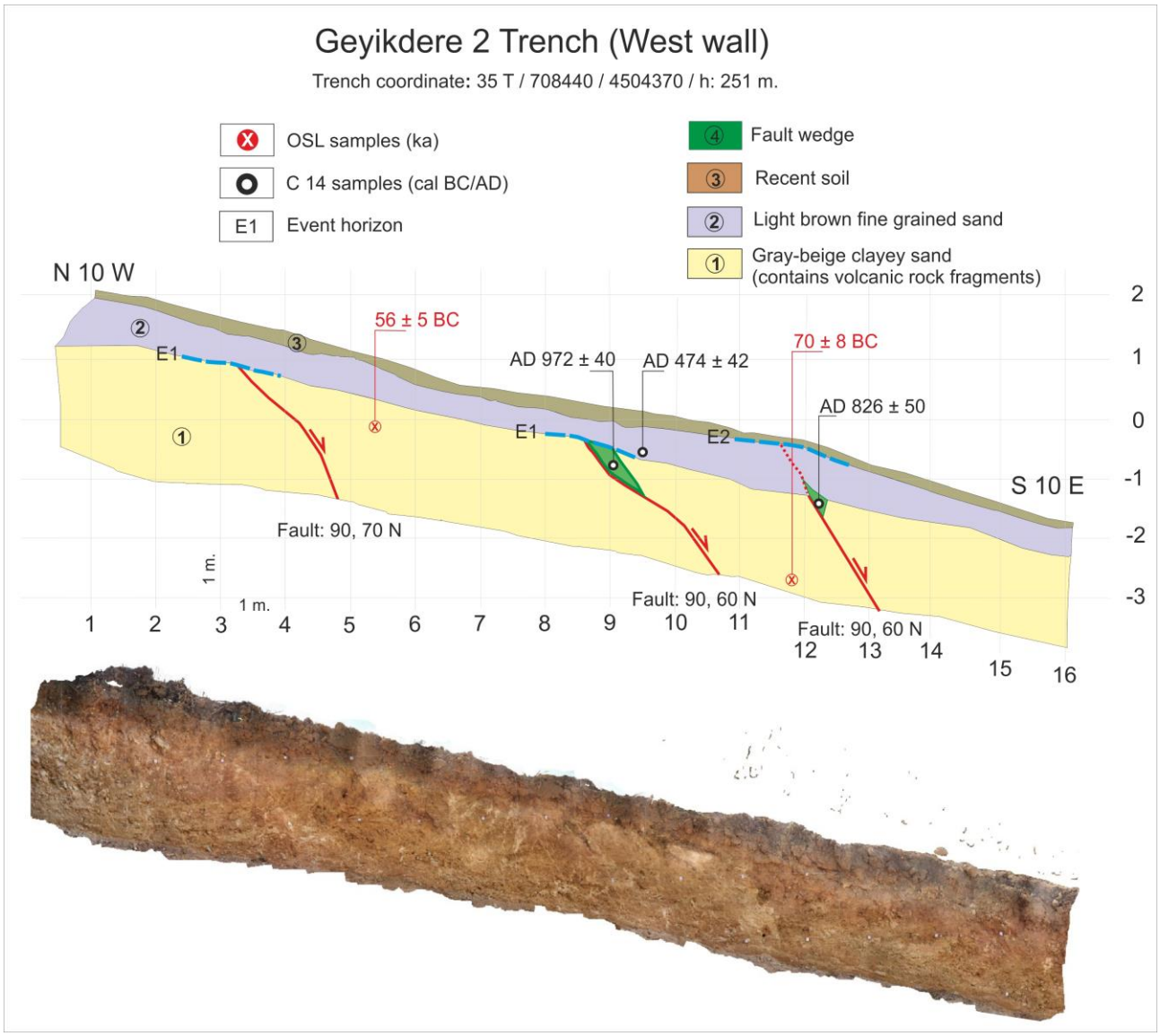


Figure 12. Log and photomosaic of Geyikdere 2 Trench.

3.1.3. Havuzdere Trenches

Three trenches were excavated at this location (UTM 35T: 708517 E / 4506169 N), situated 800 m northeast of Havuzdere village and 1100 m southeast of Çavuşçiftliği village, on the northern segment of the Altınova Fault. GPR studies were first conducted in the area where excavation was planned. Measurements were taken along a 60 m line oriented north-south. Faults were detected along the profile (Figures 13-14).

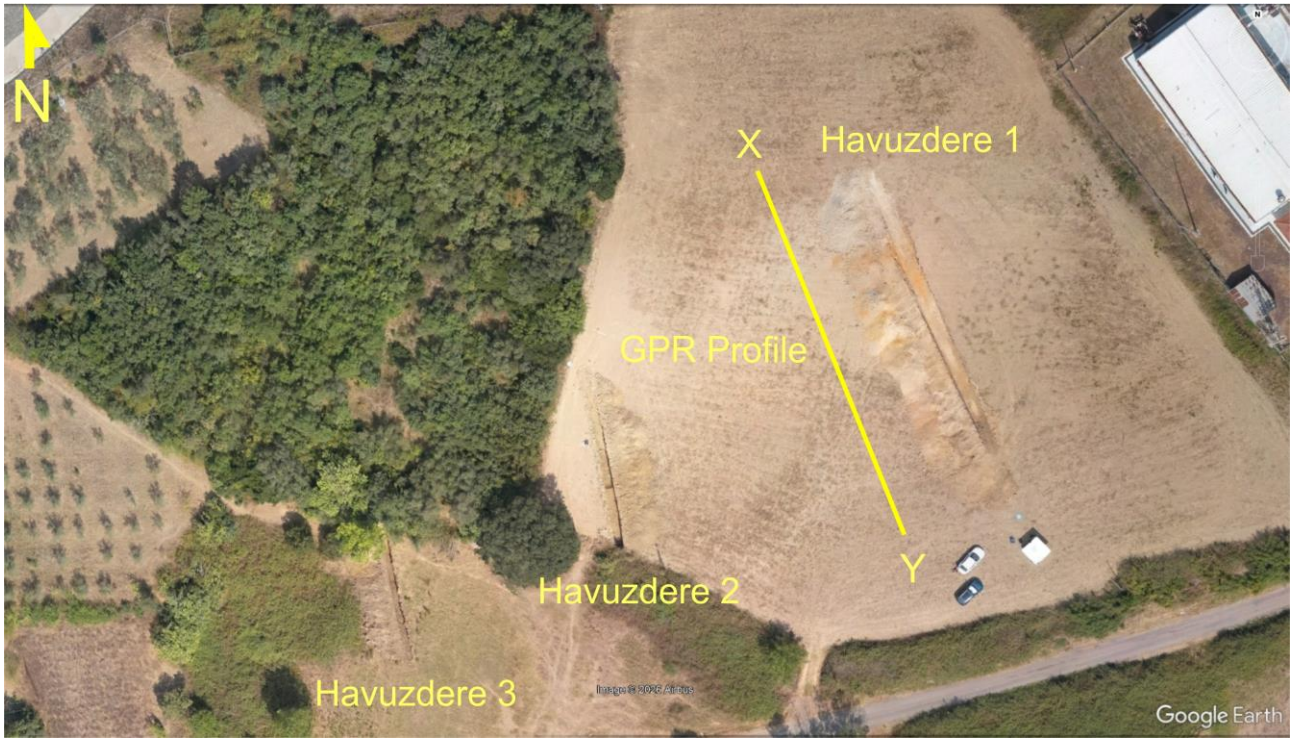


Figure 13. View of Havuzdere GPR profile and trenches.

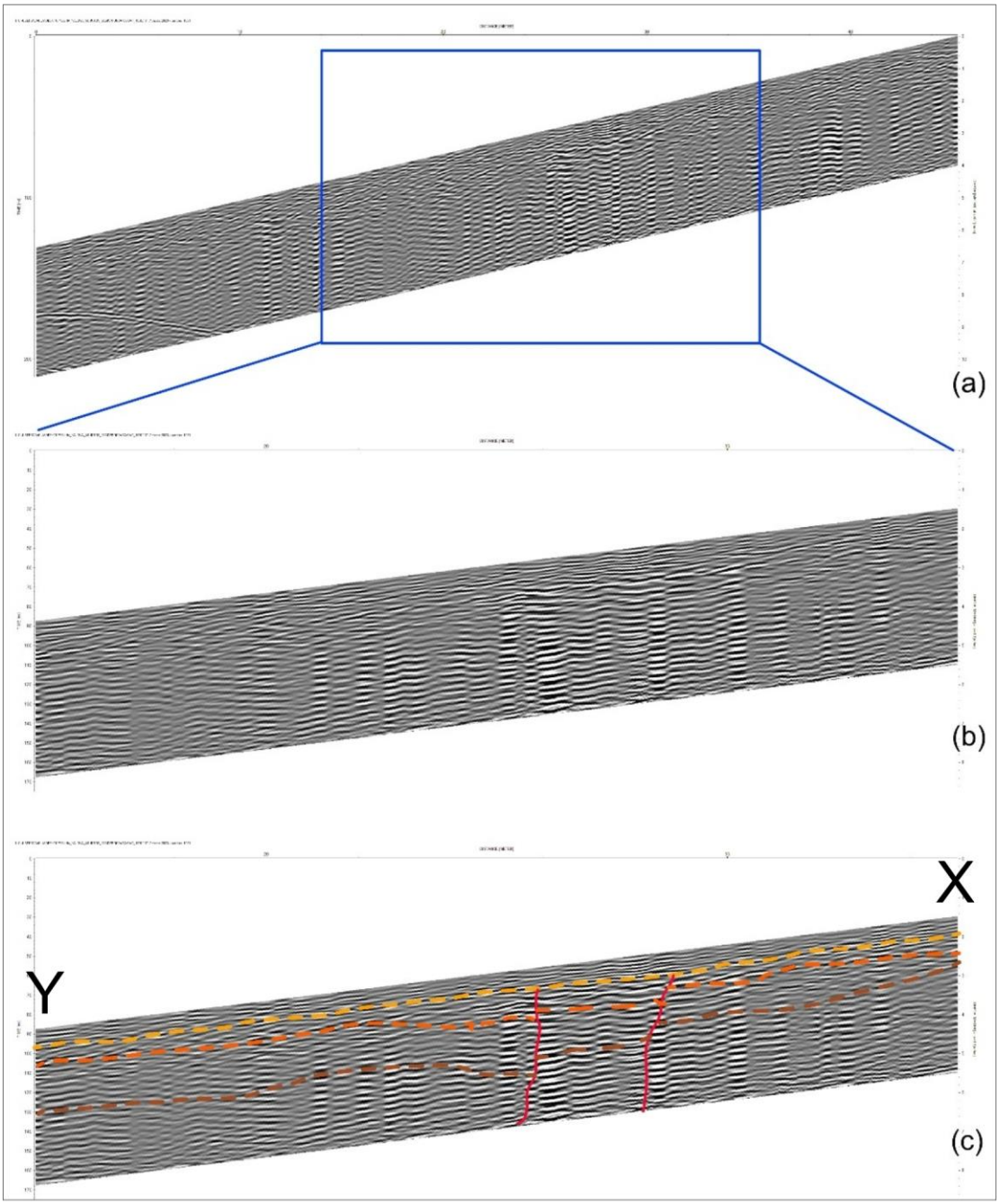


Figure 14. GPR measurements in the Havuzdere Trench area; (a) Processed GPR data (b) Anomaly region representation (c) Modeled GPR data (dashed lines indicate possible layer boundaries, red lines indicate possible discontinuity regions).

Havuzdere Trench 1 is 26 m long, 2.5 m wide and 3 m deep. Eight units, including the recent soil level, were identified in the trench walls. The bottom of the trench wall consists of gray clay (Unit 1). Above this are reddish-beige sands with fossil content (Unit 2). The sequence continues with beige, well-sorted, fine-grained sands (Unit 3) in the dip direction, followed by beige, well-sorted gravels (Unit 4). The sequence continues with a thin layer of grayish-white gravels (Unit 5) and ends with beige-light yellow fine-grained sands (Unit 6). These units, which appear to dip towards the south, are covered with recent soil (Unit 7). A sedimentary deposit (Unit 8), thought to be a fault wedge, is located 6 m from the northern end of the trench in front of the

fault. This fault is located at 70°/70° S and the second fault at the 8th meter is located at 71°/68° S. Both faults are normal faults that cause vertical displacement of the units to the south and extend to the current ground level. The displacement amount in the trench wall is observed at the lower boundary of Unit 2 and is approximately 50 cm (Figure 15).

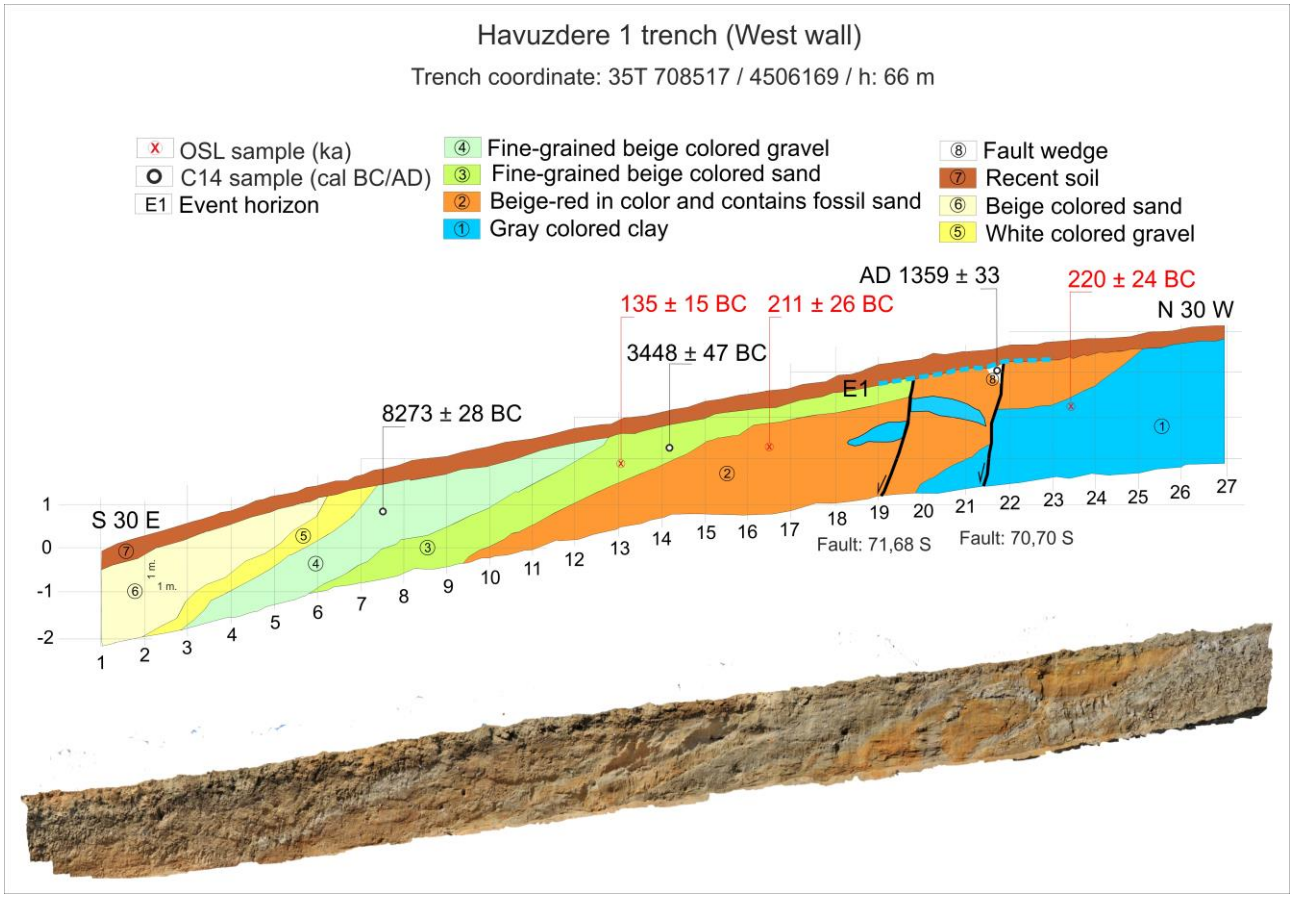


Figure 15. Log and photomosaic of Havuzdere 1 Trench.

Three samples for OSL dating and three samples for ^{14}C dating were taken to determine the earthquake occurrence times (Figure 15). An earthquake (E1 horizon) occurred between 3448 ± 47 BC and AD 1359 ± 33 according to the ^{14}C dating results from this trench. OSL (ka) data were interpreted as unit ages of 135 ± 15 BC, 211 ± 26 BC and 220 ± 24 BC.

Havuzdere Trench 2 was excavated to a length of 8 m, a width of 1.5 m and a depth of 3 m. Six units, including the recent soil level, were observed in the trench walls. Light yellow sands (Unit 1) are visible at the bottom. Above this is light brown coarse-grained sand (Unit 2). These are covered by red sands containing white caliche (Unit 3). The sequence continues upward with yellowish-gray clay (Unit 4) and is covered by the recent soil level (Unit 5). Normal faults are found on the eastern wall of the trench, located at 68°/62° S in the first meter from the north and at 73°/56° S in the second meter (Figure 16). The vertical movement visible at the base boundary of Unit 3 is approximately 1.2 m.

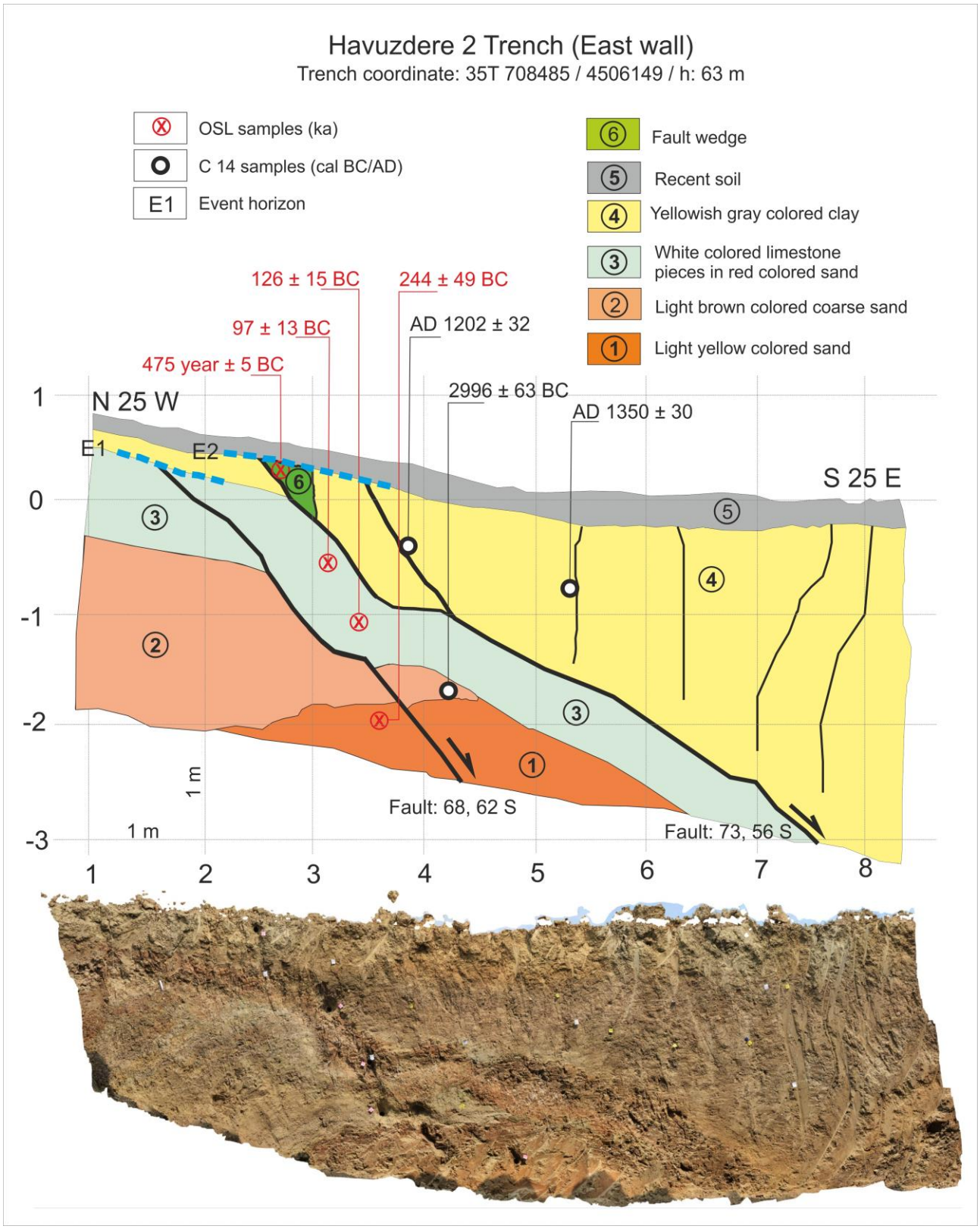


Figure 16. Log and photomosaic of Havuzdere 2 Trench.

Four samples for OSL dating and three samples for ^{14}C dating were taken from Havuzdere 2 trench to determine the timeline for paleo events. Based on the ^{14}C dating results from this trench, there may have been two earthquakes between 2996 ± 63 BC and AD 1202 ± 32 (E1 horizon) and between AD 1350 ± 30 and recent soil (E2 horizon). Based on the OSL (ka) data, unit ages were 97 ± 13 BC, 126 ± 15 BC and 244 ± 49 BC (Figure 16).

Havuzdere 3 trench was excavated to a length of 7 m, a width of 1.5 m, and a depth of 2 m. Five units were differentiated in the trench walls, along with the current soil level. At the base of the trench wall is light yellow-beige sand (Unit 1). A dark yellow coarse-grained sand layer lies conformably above this (Unit 2). The sequence continues with reddish sandstones containing white calcareous particles, and all units are covered by the recent soil level. Faults are located at 70°/69° S at the second meter from the north of the trench and at 70°/70° S at the fourth meter (Figure 17). Sediment, thought to be an earthquake deposit, is found on the fault.

Three OSL samples and two ^{14}C samples were taken to determine the interval timing of the earthquakes. Based on the ^{14}C dating results from this trench, three earthquakes may have occurred between AD 711 ± 41 and AD 1350 ± 30 (E1 horizon), AD 1350 ± 30 and AD 1875 ± 30 (E2 horizon), and between AD 1875 ± 30 and recent soil (E3 horizon). According to the OSL data (ka), the unit ages were determined to be 11 ± 10 BC, 11 ± 3 BC and 75 ± 10 BC (Figure 17).

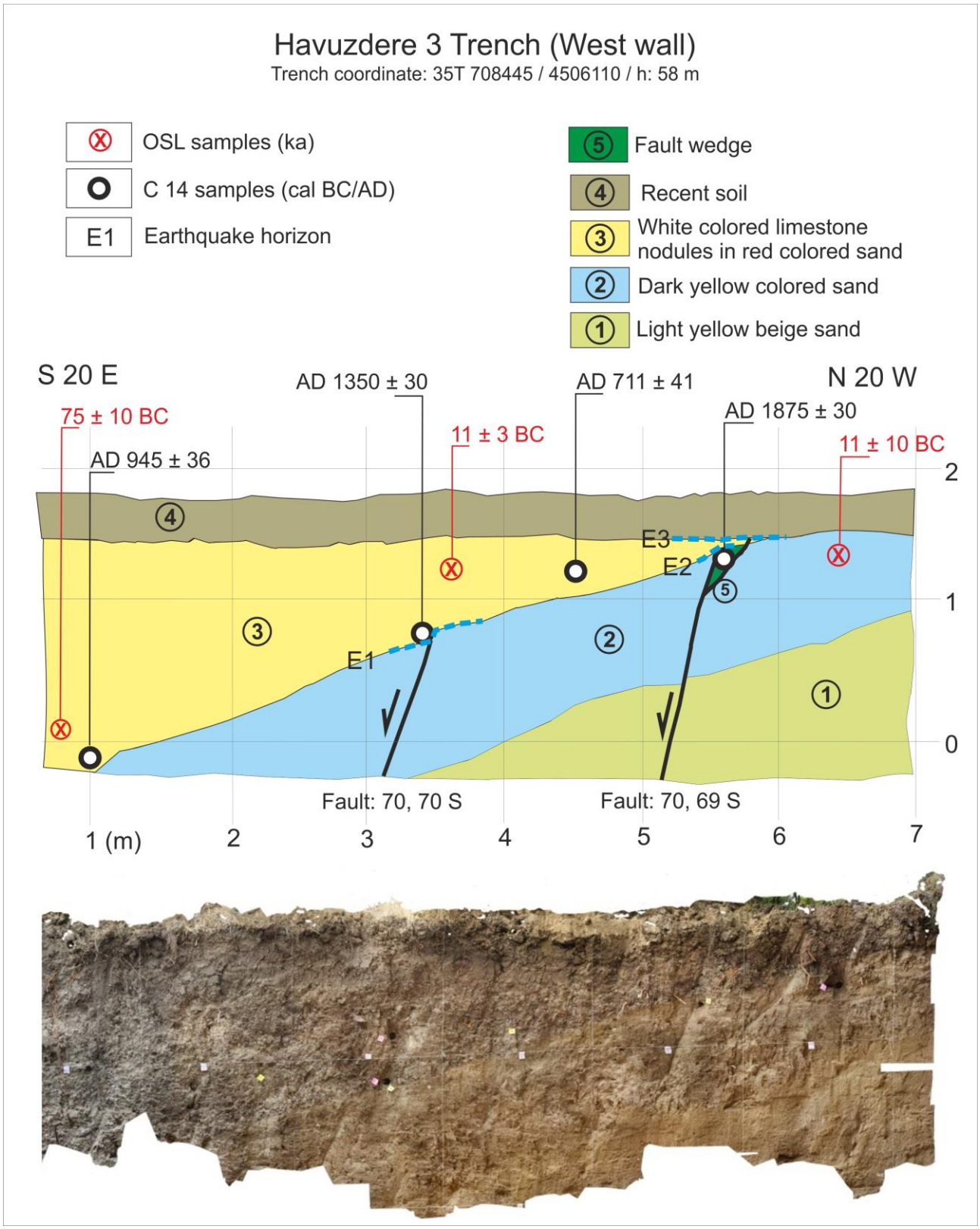


Figure 17. Log and photomosaic of Havuzdere 3 Trench.

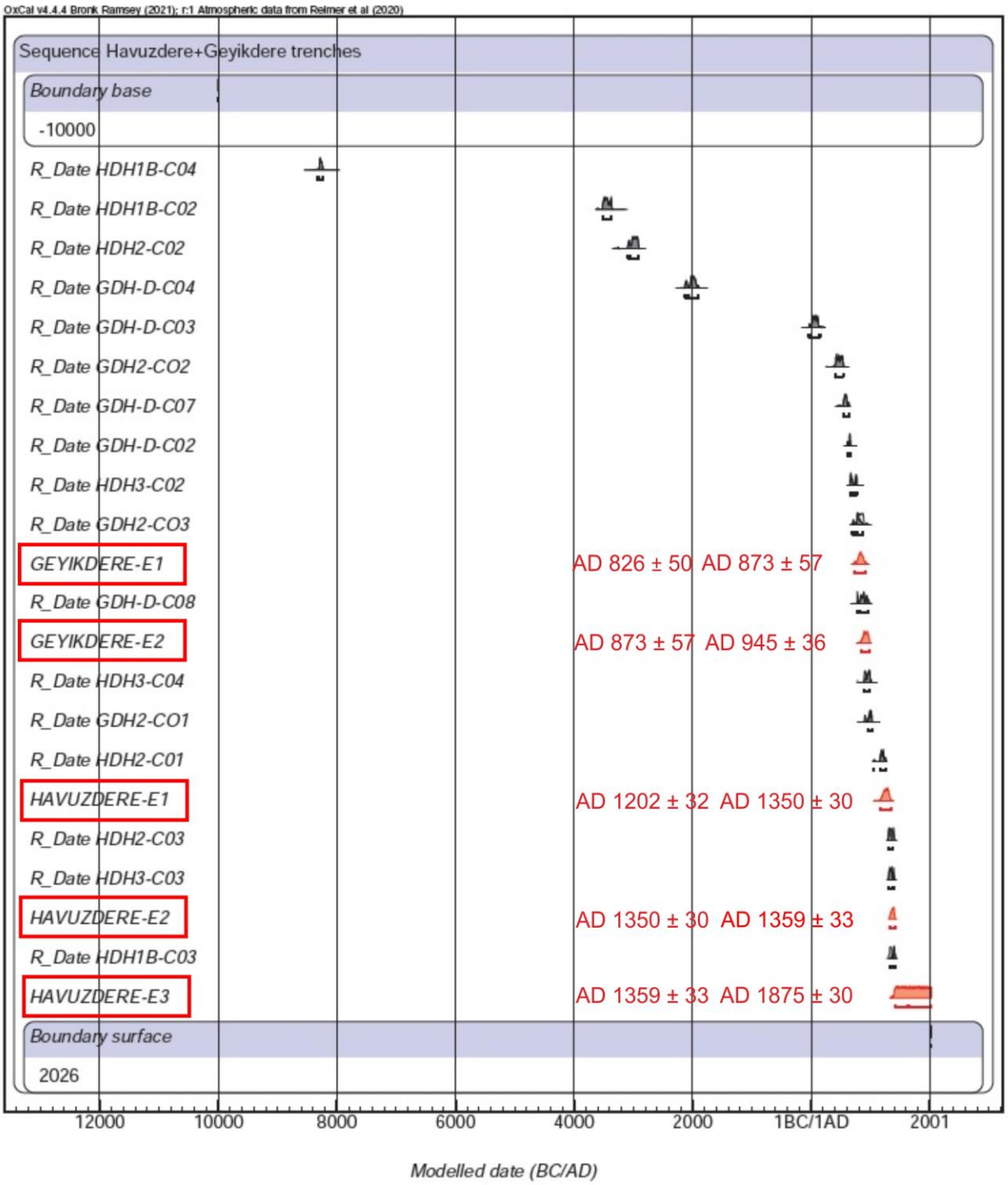


Figure 18. A comparative view of earthquake intervals established based on ^{14}C dating results falling within the Common Era (AD).

4. Discussion and Conclusion

Field observations and trench studies indicate that the NE–SW trending Altınova thrust fault was not found south of the Hersek Delta. Geological units are deformed by E–W, WNW–ESE, and NW–SE trending normal faults in both outcrops and trenches within an extensional regime. In this region, where the shear regime of the North Anatolian Fault is dominant, the normal faults documented in the Altınova trenches may represent long-lived secondary and local extensional structures that are repeatedly activated during major earthquakes on the

North Anatolian Fault system, rather than the main seismic fault itself. Although the NAFZ is predominantly a right-lateral strike-slip fault system, local extensional structures are well documented along some of its segments. Relaxation folds, steps, and secondary normal faults associated with transtensional deformation were observed during the 1999 İzmit and Düzce earthquakes and have also been identified in the Hersek Delta and the Marmara region [19, 49-50].

Paleoseismological investigations carried out in the Geyikdere and Havuzdere trenches document evidence for at least five Late Holocene surface-faulting earthquakes along the investigated sections of the Altınova Fault (Table 2; Figure 18). Event horizons were identified using multiple independent paleoseismological criteria, including upward fault terminations, colluvial wedge deposits, and stratigraphic relationships between displaced and overlying non-deformed units.

Bayesian chronological modelling using OxCal v4.4.4 [48] and the IntCal20 calibration dataset [47] provides chronological constraints for each identified event horizon. The model indicates five Late Holocene surface-faulting earthquakes. The two events recognized in the Geyikdere trenches are constrained to AD 826 ± 50 – 873 ± 57 (GD-E1) and AD 873 ± 57 – 945 ± 36 (GD-E2), whereas the three events identified at Havuzdere occurred between AD 1202 ± 32 – 1350 ± 30 (HD-E1), AD 1350 ± 30 – 1359 ± 33 (HD-E2), and AD 1359 ± 33 – 1875 ± 30 (HD-E3). The youngest event is constrained by a radiocarbon age obtained from an event-related colluvial wedge sealed beneath modern soil, demonstrating that the latest surface-faulting event predates development of the present ground surface (Figure 18).

The Bayesian chronological model suggests that the Geyikdere and Havuzdere trenches may preserve different portions of the Late Holocene paleoseismic record. Rather than defining a single continuous sequence of surface-faulting earthquakes, the identified events may reflect along-strike variations in rupture behavior, fault segmentation, or differences in sedimentation and erosion potential between the trench sites. Given the limited number of identified paleo earthquakes and the inherent uncertainties associated with trench-based records, a robust estimate of earthquake recurrence cannot be derived from the available data. Nevertheless, the results suggest that the record of surface-faulting earthquakes may not have been preserved uniformly along the investigated sections of the Altınova Fault.

The paleo earthquakes identified in the trenches broadly overlap in age with several historically documented major earthquakes in the Marmara region. The youngest event, Havuzdere-E3, is constrained to the interval between AD 1359 ± 33 and AD 1875 ± 30. Considering the chronological uncertainties, this event may tentatively be correlated with the 10 July 1894 earthquake [51-52], the 19 April 1878 earthquake [52-53], and/or the 10 September 1509 earthquake [54-55].

The Havuzdere-E2 event is constrained between AD 1350 ± 30 and AD 1359 ± 33 and falls within the chronological range of the 18 October 1343 earthquake [38]. Similarly, Havuzdere-E1 is bracketed between AD 1202 ± 32 and AD 1350 ± 30 and may correspond to the 1–13 June 1296 earthquake [38, 55].

The Geyikdere-E2 event, constrained between AD 873 ± 57 and AD 945 ± 36, may correlate with the 26 October 989 earthquake [36, 55]. Likewise, Geyikdere-E1, dated between AD 826 ± 50 and AD 873 ± 57, overlaps with the age ranges of the historically documented AD 865 and AD 875 earthquakes [36, 56].

Although the modeled event ages overlap with several historical earthquakes, these correlations remain tentative because the chronological uncertainties allow more than one possible historical counterpart for individual paleo earthquakes.

Results from the Altınova trenches reveal that deformation has been ongoing for a long duration in this area and has the potential to generate surface rupture earthquakes.

In conclusion; 5 trenches were excavated, 1 natural trench was studied and field observations were completed at 3 outcrops to reveal the earthquake history of the area south of the Hersek Delta. Accordingly:

1. In the study area, the Altınova Fault, identified in the Active Fault Map of Türkiye [25], is not a thrust fault. However, normal faults with orientations of E–W, WNW–ENE, and ENE–WSW, dipping both north and south, were identified in all trenches and outcrops. It is concluded that these normal faults are local normal faults [50] that developed under an extensional regime with orientation of approximately NNE–SSW.

2. In all excavations, earthquake traces and wedges, particularly those potentially related to faults, were sought, and as a result, the presence of multiple earthquakes was detected.

3. A total of 21 samples from 6 trenches were analyzed using ^{14}C and OSL dating methods. ^{14}C data defined five different earthquake time intervals in the trenches. Ages of the stratigraphic units in trenches have been determined by OSL data.

4. This suggests that these detected earthquakes may not be unique to this region but may have occurred during earthquakes on the NAFZ or other fault segments in the surrounding area.

5. This initial paleoseismological study will guide future studies in this region, providing insights into new earthquakes and the recurrence interval of earthquakes in this area.

Author Contributions

All authors equally contributed to this paper. They have all read and approved the final version of the paper.

Declaration

This paper is derived from the first author's doctoral dissertation supervised by the second author.

Conflict of Interest

All the authors declare no conflict of interest.

Ethical Review and Approval

No approval from the Board of Ethics is required.

Artificial Intelligence (AI) Use Statement

The authors declare that no artificial intelligence (AI) tools were used in any part of the study or in the preparation of this manuscript.

Acknowledgment

This study was carried out within the scope of TÜBİTAK KAMAG 1007 project number 123G013 for MTA (Mineral Research and Exploration Institute in Türkiye), the client institution. We thank the editors and reviewers who evaluated the article for their valuable critiques and TÜBİTAK for their contribution. The authors would like to thank Catherine Yiğit for professional editing assistance with English that improved the final version of the text.

References

[1] D. McKenzie, *Active tectonics of the Mediterranean region*, Geophysical Journal of the Royal Astronomical Society 30 (2) (1972) 109–185. [link]

[2] D. McKenzie, *Some remarks on the development of sedimentary basins*, Earth and Planetary Science Letters 40 (1978) 25–32. [link]

[3] M. C. Şengör, *The North Anatolian transform fault: its age, offset and tectonic significance*, Journal of the Geological Society 136 (3) (1979) 269–282. [link]

[4] X. Le Pichon, J. Angelier, *The Aegean Sea*, Philosophical Transactions of the Royal Society of London, Series A, Mathematical and Physical Sciences 300 (1454) (1981) 357–372. [link]

[5] M. C. Şengör, Y. Yılmaz, *Tethyan evolution of Turkey: a plate tectonic approach*, Tectonophysics 75 (1981) 181–241. [link]

[6] J. Jackson, D. McKenzie, *Active tectonics of the Alpine–Himalayan belt between western Turkey and Pakistan*, Geophysical Journal of the Royal Astronomical Society 77 (1) (1984) 185–264. [link]

[7] J. Dewey, M. L. Helman, S. D. Knott, E. Turco, D. H. W. Hutton, *Kinematics of the western Mediterranean*, Geological Society, London, Special Publications 45 (1) (1989) 265–283. [link]

[8] R. Westaway, *Present-day kinematics of the Middle East and eastern Mediterranean*, Journal of Geophysical Research 99 (B6) (1994) 12071–12090. [link]

[9] Barka, *The North Anatolian fault zone*, Annales Tectonicae 6 (1992) 164–195. [link]

[10] M. C. Şengör, N. Görür, F. Şaroğlu, *Strike-slip faulting and related basin formation in zones of tectonic escape: Turkey as a case study,* Strike-Slip Deformation, Basin Formation, and Sedimentation, Vol. 37 of SEPM Special Publication, Society for Sedimentary Geology, 1985, pp. 227–264. [link]

[11] Özkan, H. H. Yavaşoğlu, İ. Tiryakioğlu, G. Uslular, M. F. Karabulut, P. Ulrich, F. Masson, *New GPS-derived velocity field for Marmara region: Implications for the kinematics along the North Anatolian Fault Zone*, Tectonics 911 (2025) 230828. [link]

[12] R. Reilinger, S. McClusky, P. Vernant, S. Lawrence, S. Ergintav, R. Cakmak, H. Özener, F. Kadirov, I. Guliev, ..., G. Karam, *GPS constraints on continental deformation in the Africa-Arabia-Eurasia continental collision zone and implications for the dynamics of plate interactions*, Journal of Geophysical Research: Solid Earth, 111 (2006) B05411. [link]

[13] S. McClusky, S. Balassanian, A. Barka, C. Demir, S. Ergintav, I. Georgiev, O. Gurkan, M. Hamburger, K. Hurst, ..., G. Veis, *Global Positioning System constraints on plate kinematics and dynamics in the eastern Mediterranean and Caucasus*, Journal of Geophysical Research: Solid Earth, 105 (B3) (2000) 5695–5719. [link]

[14] J. Meade, B. H. Hager, S. McClusky, R. E. Reilinger, S. Ergintav, O. Lenk, A. Barka, H. Özener, *Estimates of seismic potential in the Marmara Sea region from block models of secular deformation constrained by Global Positioning System measurements*, Bulletin of the Seismological Society of America, 92 (1) (2002) 208–215. [link]

[15] S. Özalp, Ö. Emre, A. Doğan, *The segment structure of southern branch of the North Anatolian Fault and paleoseismological behaviour of the Gemlik Fault, NW Anatolia*, Bulletin of the Mineral Research and Exploration, 147 (2013) 1–17. [link]

[16] R. S. Stein, A. A. Barka, J. H. Dieterich, *Progressive failure on the North Anatolian fault since 1939 by earthquake stress triggering*, Geophysical Journal International, 128 (3) (1997) 594–604. [link]

[17] T. Parsons, R. S. Stein, R. W. Simpson, P. A. Reasenberg, *Stress sensitivity of fault seismicity: A comparison between limited-offset oblique and major strike-slip faults*, Journal of Geophysical Research: Solid Earth, 104 (B9) (1999) 20183–20202. [link]

[18] M. Erdik, M. Demircioglu, K. Sesetyan, E. Durukal, B. Siyahi, *Earthquake hazard in Marmara region, Turkey*, Soil Dynamics and Earthquake Engineering, 24 (8) (2004) 605–631. [link]

[19] Barka, H. S. Akyuz, E. Altunel, G. Sunal, Z. Cakir, A. Dikbas, B. Yerli, R. Armijo, B. Meyer, ..., W. Page, *The surface rupture and slip distribution of the 17 August 1999 Izmit earthquake (M 7.4), North Anatolian fault*, Bulletin of the Seismological Society of America, 92 (1) (2002) 43–60. [link]

[20] W. Lettis, J. Bachhuber, R. Witter, C. Brankman, C. E. Randolph, A. Barka, W. D. Page, A. Kaya, *Influence of releasing step-overs on surface fault rupture and fault segmentation: Examples from the 17 August 1999 Izmit earthquake on the North Anatolian fault, Turkey*, Bulletin of the Seismological Society of America, 92 (1) (2002) 19–42. [link]

[21] Ö. Kozacı, *Paleoseismological Studies on the Yalova Segment of the North Anatolian Fault in the Hersek Delta,* Master's Thesis İstanbul Technical University (2002) İstanbul. [link]

[22] R. Demirtaş, Hersek *(Altınova) Delta paleoseismological studies*, General Directorate of Disaster Affairs (2007). [link]

[23] V. Özaksoy, Ö. Emre, C. Yıldırım, A. Doğan, S. Özalp, F. Tokay, *Sedimentary record of late Holocene seismicity and uplift of Hersek restraining bend along the North Anatolian Fault in the Gulf of İzmit*, Tectonophysics 487 (1-4) (2010) 33–45. [link]

[24] Ö. Kozacı, E. Altunel, S. Lindvall, C. Brankman, W. Lettis, *The North Anatolian fault on the Hersek Peninsula, Turkey: Its geometry and implications for the 1999 Izmit earthquake rupture propagation*, Turkish Journal of Earth Sciences, 20 (4) (2011) 359–378. [link]

[25] Ö. Emre, A. Doğan, T. Y. Duman, S. Özalp, 1: 250,000 scale Active Fault Map Series of Turkey, Bursa (NK 35-12) Quadrangle, General Directorate of Mineral and Exploration, Ankara-Türkiye, Serial Number: 9 (2011) Accessed: 13 Feb 2026. [link]

[26] Ö. Emre, T. Y. Duman, S. Özalp, F. Şaroğlu, Ş. Olgun, H. Elmacı, T. Çan, *Active fault database of Turkey*, Bulletin of Earthquake Engineering, 16 (8) (2018) 3229-3275. [link]

[27] Elmas, E. Yiğitbaş, *Ophiolite emplacement by strike-slip tectonics between the Pontide Zone and the Sakarya Zone in northwestern Anatolia, Turkey*, International Journal of Earth Sciences, 90 (2) (2001) 257-269. [link]

[28] Y. Yılmaz, O. Tüysüz, E. Yiğitbaş, Ş. C. Genç, A. M. C. Şengör, *Geology and tectonic evolution of the Pontides*, Regional and Petroleum geology of the Black Sea and Surrounding Region, Vol. 68 of AAPG Memoir, American Association of Petroleum Geologists, 1997, pp. 183–226. [link]

[29] E. Yiğitbaş, A. Elmas, Y. Yılmaz, *Pre-Cenozoic tectono-stratigraphic components of the western pontides and their geological evolution*, Geological Journal, 34 (1-2) (1999) 55-74. [link]

[30] Ö. Emre, T. Erkal, A. Tchepalyga, N. Kazancı, M. Keçer, E. Ünay, *Neogene-Quaternary evolution of the eastern Marmara region, northwest Turkey*, Bulletin of the Mineral Research and Exploration, 120 (1998) 119-145. [link]

[31] S. Bargu, M. Sakınç, *Geology and structural features of the region between Izmit Bay and Iznik Lake,* Istanbul University Faculty of Engineering Journal of Earth Sciences, 7 (1-2) (1990) 45-76. [link]

[32] S. Bargu, M. Sakınç, *Investigation and Evaluation of Natural Aggregate Potential of the Section Between Karamürsel and İznik Lake in Armutlu Peninsula*, TÜBİTAK TBAG-587 Report, Ankara, 1984. [link]

[33] M. Albayrak, A. Kahya, *Mineralogical and Petrographic Characteristics of Zeolitic Tuffs Around Havuzdere, Geyikdere, İnebeyli and Tepeköy (Karamürsel, Yalova, Türkiye),* Dicle University Faculty of Engineering Engineering Journal,15 (1) (2024) 177–190. [link]

[34] N. Ambraseys, *The seismic activity of the Marmara Sea region over the last 2000 years*, Bulletin of the Seismological Society of America, 92 (1) (2002) 1-18. [link]

[35] N. N. Ambraseys, *The earthquake of 1509 in the Sea of Marmara, Turkey, revisited*, Bulletin of the Seismological Society of America, 91 (6) (2001) 1397-1416. [link]

[36] E. Guidoboni, A. Comastri, G. Traina, Catalogue of Ancient Earthquakes in the Mediterranean Area up to 10th Century, Ist. Naz. di Geofis. e Vulcanol., Storia Geofis. Ambiente, Bologna, Italy, 1994. [link]

[37] N. N. Ambraseys, C. F. Finkel, The Seismicity of Turkey and Adjacent Areas a Historical Review, 1500-1800, Eren Yayınevi, İstanbul, 1995. [link]

[38] E. Guidoboni, A. Comastri, Catalogue of earthquakes and tsunamis in the Mediterranean area from the 11th to the 15th century, INGV-SGA, Bologna, Italy, 2005. [link]

[39] J. L. Davis, A. P. Annan, *Ground-penetrating radar for high-resolution mapping of soil and rock stratigraphy*, Geophysical Prospecting, 37 (5) (1989) 531-551. [link]

[40] C. Yalçıner, B. Alpar, Y. Altınok, İ. Özbay, F. Imamura, *Tsunamis in the Sea of Marmara Historical documents for the past, models for the future*, Marine Geology, 190 (1-2) (2002) 445-463. [link]

[41] L. B. Conyers, Ground-penetrating radar for archaeology, Encyclopedia of imaging science and technology, 2004. [link]

[42] Ç. Balkaya, G. Göktürkler, *Modeling of through-well ground radar data,* Pamukkale University Journal of Engineering Sciences, 22 (6) (2016) 581-596. [link]

[43] L. Becerra-Valdivia, T. Higham, New developments in radiocarbon dating, Handbook of Archaeological Sciences, 2023, pp. 25-35. [link]

[44] Baral, S. Budhathoki, A. Bhattarai, N. K. Chaudhary, *Revolutionizing Age Determination: Theoretical Insights into Radiocarbon (^{14}C) Dating*, Contemporary Research: An Interdisciplinary Academic Journal, 7 (2) (2024) 77-95. [link]

[45] M. Chen, D. W. Li, H. Zhang, Z. Wang, M. Zhao, *Distinct variations and mechanisms for terrestrial OC ^{14}C-ages in the Eastern China marginal sea sediments since the last deglaciation*, Quaternary Science Reviews, 315 (2023) 108235. [link]

[46] J. Rhodes, *Optically stimulated luminescence dating of sediments over the past 200,000 years*, Annual Review of Earth and Planetary Sciences, 39 (1) (2011) 461-488. [link]

[47] P. J. Reimer, M. G. L. Baillie, E. Bard, A. Bayliss, J. W. Beck, C. J. H. Bertrand, P. G. Blackwell, C. E. Buck, G. Burr, …, C. E. Weyhenmeyer, *IntCal04 terrestrial radiocarbon age calibration, 0-26 cal kyr BP*, Radiocarbon, 46 (3) (2004) 1029-1058. [link]

[48] Bronk Ramsey, OxCal v.4.4.4 (2021). Accessed 26 Sep 2026. [link]

[49] Ö. Kozacı, J. F. Dolan, R. C. Finkel, R. D. Hartleb, *Late Holocene slip rate for the North Anatolian fault, Turkey, from cosmogenic ^{36}Cl geochronology: Implications for the constancy of fault loading and strain release rates*, Geology, 35 (10) (2007) 867–870. [link]

[50] S. Özden, S. Över, S. Altuncu Poyraz, Y. Güneş, A. Pınar, *Tectonic implications of the 2017 Ayvacık (Çanakkale) earthquakes, Biga Peninsula, NW Turkey*, Journal of Asian Earth Sciences, 154 (2018) 125-141. [link]

[51] Öztin, *1894 İstanbul Depremi Raporu*, Bayındırlık ve İskân Bakanlığı Afet İşleri Genel Müdürlüğü Deprem Araştırma Dairesi, Ankara, 1994. [link]

[52] N. N. Ambraseys, A. Zatopek, *The Mudurnu Valley, West Anatolia, Turkey, earthquake of 22 July 1967*, Bull. Seism. Soc. Am., 59 (1969) 521-589. [link]

[53] A. Zachariadou, Doğal Afetler: Fırsat Anları. Osmanlı İmparatorluğu'nda Doğal Afetler, Tarih Vakfı Yurt Yayınları, İstanbul, 2001, pp. 6-10. [link]

[54] Öztüre, Resim, Fotograf ve Belgelerle Nicomedia İzmit tarihi, Çeltüt Matbaası, İstanbul, 1969. [link]

[55] N. Ambraseys, Earthquakes in the Mediterranean and Middle East: a multidisciplinary study of seismicity up to 1900, Cambridge University Press, Cambridge, 2009. [link]

[56] Soysal, S. Sipahioğlu, D. Kolçak, Y. Altınok, *Historical Earthquake Catalogue of Turkey and Surrounding Area (2100 B.C.-1900 A.D.),* Technical Report No. TBAG-341, TÜBİTAK, İstanbul, 1981. [link]